"Evidence for Electrolytically Induced Transmutation and Radioactivity Correlated with Excess Heat in Electrolytic Cells With Light Water Rubidium Salt Electrolytes"*

R. Bush and R. Eagleton
Physics Department, California State Polytechnic University
3801 W. Temple Avenue
Pomona, California 91768
(909) 869-4018
and
ENECO**

Abstract

Two separate mass spectrometric analyses, SIMS and ICPMS of 1.0 amu discrimination , performed by two independent laboratories on the pre-run and post-run cathode material from a light water based rubidium carbonate cell and a rubidium hydroxide cell provide strong evidence for the electrolytically induced transmutation of rubidium to strontium originally hypothesized by Bush in connection with his CAF hypothesis ("Cold Alkali Fusion"). The SIMS analysis showed that the abundance ratio of Sr86 to Sr 88shifted from the normal abundance ratio of about 0.12 in the prerun cathode sample to essentially the same value, 2.6, as the natural abundance ratio of Rb85 to Rb87, where the latter are the respective parent isotopes hypothesized by Bush. Proof that this shift by a factor of about 22 from the natural abundance ratio for the strontium isotopes could not have been a spurious SIMS result due to rubidium hydride formation was demonstrated by additional mass spectroscopy, ICPMS, preceded by an ion-exchange column separation of the strontium and the rubidium. In the ICPMS tests, the postrun cathode material from both cells demonstrated a shift in the strontium isotope abundance ratio by an amount that is more than 600 standard deviations away from the normal ratio (prerun sample). In addition, for a third rubidium carbonate cell, strong preliminary evidence is presented for electrolytically induced radioactivity. The experimental work provides strong initial support for Bush's LANT hypothesis ("Lattice Assisted Nuclear Transmutation").

Introduction

Analyses of the pre-run electrode material and post-run electrodes from two light water based rubidium salt electrolytic cells, cell 53 (rubidium carbonate) and cell 56 (rubidium hydroxide) having nickel mesh cathodes by two independent laboratories provide strong initial evidence in support of Bush's CAF Hypothesis[1,6] ("Cold Alkali Fusion") that strontium is being produced from rubidium via a cold nuclear reaction in which a proton is being added to Rb^{85} (Rb^{87}) to produce Sr^{86}(Sr^{88}). The postrun cathode material of cell 53 was analyzed via SIMS, while that for cell 53 and cell 56 was analyzed via Inductively Coupled Mass Spectrometry (1 amu discrimination) following an ion exchange column enhancement of the strontium relative to the rubidium[1,2,6] at WCAS (" West Coast Analytical Service, Inc. ") of Santa Fe Springs, CA. For an additional rubidium carbonate cell, cell 71, there is initial evidence for electrolytically induced radioactivity. A scintillation tube combined with a multi-channel analyzer was employed to establish a radioactive decay curve corresponding to an average half-life of about 3.8 days. This result combined with the earlier mass spectrometric evience and its correlation with the excesss heats measured via calorimetry provides support for Bush's LANT ("Lattice Assisted Nuclear Transmutation") hypothesis[3] according to which a cold nucleosynthetic chain extending beyond strontium production is revealed for the light water rubidium electrolytic cells.

Cell Design and Calorimetry

The cell and calorimeter design employed for the present series of experiments were of two types: (1) Cells 53 and 56 were essentially the same as that reported in Ref. 2. which was a modified Fleishmann-Pons (Ref. 4) electrolytic cell with the following principal modifications: (a) the use of a *platinum black recombiner* in the cell to allow for *closed-cell operation,* (b) a *magnetic stirrer* that provided for more uniform electrolyte mixing, and (c) *Teflon* coating of all nonelectrode materials to reduce electrolyte contamination. Cell 71 was of a single wall construction and is described in another paper (ref. 4).

The electrolytic cells, as shown in Fig. 1, consisted of double wall pyrex vessels surrounded by a one inch thick layer of styrofoam. Cell temperature was regulated by controlling the temperature of the bath water which flowed through the jacket surrounding the cell. Data on cell temperatures, current, and voltage were monitored and logged by a MacIntosh IIx computer equipped with National Instrument's LabView software. Four type K thermocouples were used with each cell: one at the bath inlet port, one at the bath outlet port, and two within the electrolytic cell. The thermocouple voltages were converted to temperature by use of AD595AQ/9217 integrated circuit chips. This system permitted steady state temperature measurements with standard deviations of about 0.05 ^{o}C. Corrections for thermocouple temperature offsets were made within the software. Current and voltage signals were logged from Fluke 45 dual display multimeters which were equipped with IEEE bus.

FIGURE 1:

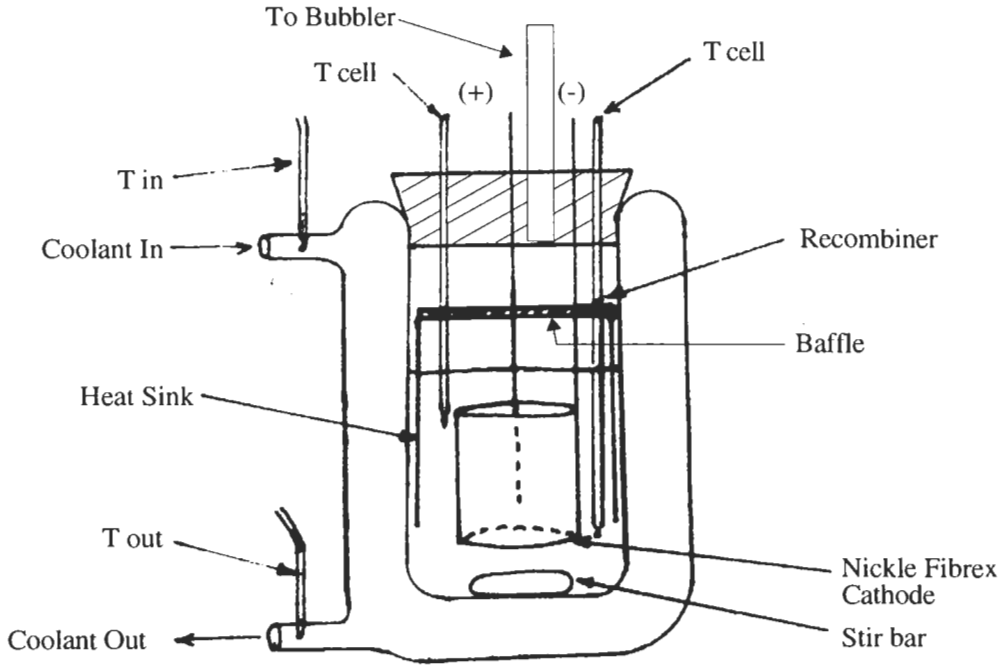

PRINCIPAL FEATURES

- Closed Cell Operation
- Mechanically Stirred Electrolyte
- Recombiner Baffle & Heat Sink
- Teflon Cell
- Platinum Anode
- Nickel Fibrex Cathode
- Nanopure H_2O Base Electrolyte
- Constant Coolant Flow Rate
- Constant Current And Temperature Operation

Pertinent details for the cells of interest in this report are as follows:

Cell #	Cathode	Anode	I mA/cm^2	Electrolyte
53	Nickel Sponge, 45 cm^2	Pt	1.0	0.57M Rb_2CO_3 50 ml
56	Nickel Sponge, 45 cm^2	Pt	1.0	0.57M RbOH 45 ml
71	Nickel Sponge, 55 cm^2	Pt	1.0	0.57 M Rb_2CO_3 65ml

Here the charging current density for the cells is given in the column headed by "I mA/cm^2". Anodic calibration was used for all cells.

The cells were calibrated by determining the steady-state temperature difference across the cell walls as a function of the electrical power supplied to the cell while running anodically. Since the thermal power out of the cell must equal the electrical power into the cell when it is in steady-state, one can use the calibration curve to determine the thermal power out of the cell for a given average temperature drop across the cell wall. The average temperature drop across the cell wall is found by taking the average of the inlet and outlet bath temperatures and subtracting this from the average of the two cell thermocouples. Excess power production was obtained by subtracting the electrical power supplied to the cell from the thermal power flowing from the cell.

SIMS Results for Postrun Cathode of Cell 53

A SIMS analysis for the post-run cathode material of cell #53 showed strong lines at mass numbers 86 and 88 that were not present in the pre-run spectrum[1,2,6]. Figures 2 through 5 portray the four mass spectrograms, respectively: Postrun cathode material: 0-100 amu, Prerun: 0-100 amu, Postrun: 100-200 amu, and Postrun: 0-100 amu.

FIGURE 2. Cathode post-run mass spectrogram.

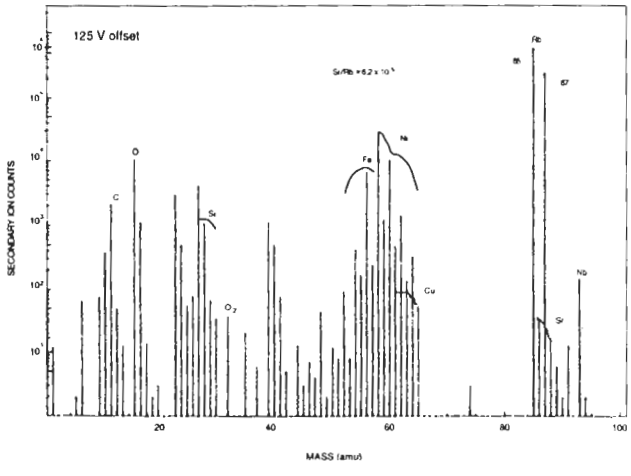

FIGURE 3. Cathode pre-run mass spectrogram.

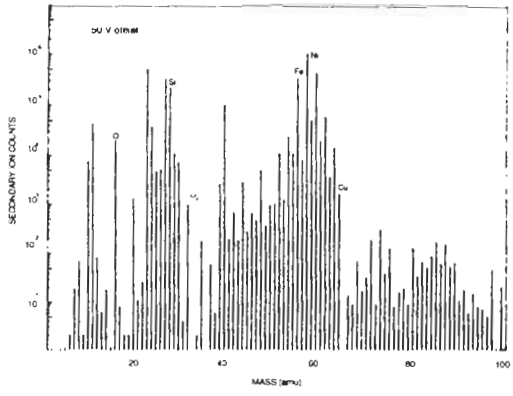

FIGURE 4. Cathode post-run mass spectrogram.

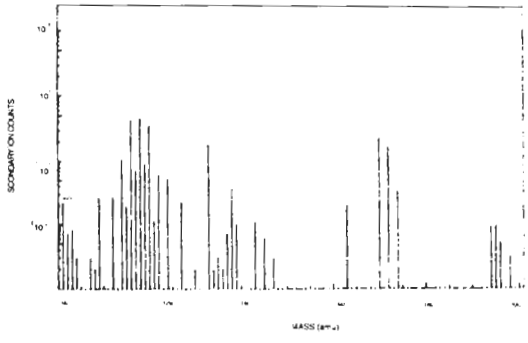

FIGURE 5. Cathode pre-run mass spectrogram.

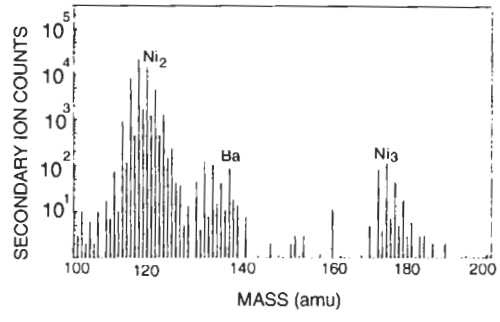

Appendix A provides an interpretation of these from the standpoint of hpothetical strontium production. An interesting finding from the standpoint of the CAF Hypothesis[1,3,6] is the fact that, within experimental

error, the ratio of the line height for mass number 86 to that for 88 was the same as that for the ratio of the rubidium signals at masses 85 and 87. (The SIMS tests were performed under the auspices of a wellknown U.S. National Laboratory, which because of the present political atmosphere for cold fusion work, prefers not to have their name revealed at this time.)

A disadvantage of these SIMS tests was that the mass spectrometer employed was unable to discriminate between rubidium hydride and strontium; i.e., $Rb^{85}H$ would be indistinguishable from Sr^{86}. So, even though there was strong evidence pointing to the noninvolvement of rubidium hydride, such as the instability of the latter and the fact that the rubidium oxide lines, which should have been higher than those for RbH because of the greater stability of RbO, were shorter than those for the putative RbH, it was decided to pursue additional tests in which a chemical separation of the rubidium and strontium would first be performed prior to the mass spectrometric analysis. These analyses were carried out by West Coast Analytical Services, Inc., of Santa Fe Springs, CA.

Ion Column Exchange Separation of the Rubidium and Strontium Followed by ICPMS ("Inductively-Coupled Plasma Mass Spectroscopy") (Cells 53, 56)

Since, at least in priciple, criticism could be levelled at the SIMS results by suggesting the formation of RbH to account for an apparent strong enhancement of Sr86 to Sr88 it was decided to have an ICPMS ("Inductively Coupled Plasma Mass Spectrometry") analysis performed at an independent laboratory, West Coast Analytical Service, Inc.[1,2](Hereafter: WCAS) of Santa Fe Springs, CA. Two pages of their final report is included as Appendix B. Because the mass discrimination of the spectrometer was limited to one amu, they first performed an ion-exchange column separation to concentrate the divalent strontium relative to the monovalent rubidium, which was washed selectively out of the column.

A summary of the WCAS results is included in the Table of Fig. 6. Previously WCAS had found that the virgin cathode material gave readings for the relative percentages of the two strontium isotopes of interest essentially the same as that of the Strontium Standard average given in the data table of Fig. 6 as follows: Sr 86: (10.51 ± 0.04)% and Sr 88: (89.49 ± 0.04)%. This gives a ratio of Sr 88 to Sr 86 for the standard (and vigin cathode material) of (8.515 ± 0.004) to which the ratios for the postrun cathode material will next be compared. From the data summary in Fig. 6, the following results are seen for the post-run cathode material of cell 53 (Sample A#53) for the test date of (4/9/93): Sr 86: (22.20 ± 0.05)% and Sr 88: (77.80 ± 0.05)%. The ratio of Sr 88 to Sr 86 is thus (3.504 ± 0.002), which is lower than the ratio for the virgin material by about 716 standard deviations as seen by the following: (8.515 - 3.504)/ (0.007) = 715.8. Since the ratio was reduced from that of the standard (virgin cathode material), this provides good evidence for an enhancement of Sr 86 relative to Sr 88 for the postrun cathode of cell 53, a light water based rubidium carbonate cell. For cell 56 (light water based rubidium hydroxide), which had evidenced about five times as much excess heat as cell 53 based upon calorimetry, the data table of Fig. 6 gives results for the analysis of sample #56PR on (4/9/93) as follows: Sr 86: (26.80 ± 0.05)% and Sr 88: (73.20 ± 0.05)%. The following ratio of Sr 88 to Sr 86 for these numbers implies an even greater electrolytically induced enhancement of Sr 86 relative to Sr 88, which could be anticipated based upon the greater excess heat exhibited by cell 56: (2.731 ± 0.003). Again, as dramatic evidence for this enhancement of Sr 86 relative ro Sr 88 this ratio is less than the standard by about 826 standard deviations as seen by the following: (8.515 - 2.731)/ (0.007) = 826.3. Thus these ICPMS results of WCAS obtained by first achieving a chromatographic concentration of the strontium relative to the rubidium provide strong independent support for the SIMS results.

Figure 6

WEST COAST ANALYTICAL SERVICE, INC.

C.S.P.U.
Dr. Robert T. Bush

Job # 23653
April 22, 1993

LABORATORY REPORT

Table 1

Date	Sample ID	Sr 86	Sr 88	Total Strontium
4-8-93	0.01ppm Sr Std	10.48	89.52	10ppb
4-9-93	0.01ppm Sr Std	10.48	89.52	10ppb
4-13-93	0.01ppm Sr Std	10.56	89.44	10ppb
4-14-93	0.01ppm Sr Std	10.53	89.47	10ppb
		10.51±0.04	89.49±0.04	

Date	Sample ID	Sr 86	Sr 88	
4-13-93	100ppm Rb/0.01ppm Sr.	10.47	89.53	10ppb
4-15-93	100ppm Rb/0.01ppm Sr.	10.55	89.45	10ppb
		10.51±0.06	89.49±0.06	

Date	Sample ID	Sr 86	Sr 88	
4-8-93	A#53	ND	ND	ND
4-9-93	A#53	22.2	77.8	1400ppb
4-15-93	A#53	12.05	87.95	NC

Date	Sample ID	Sr 86	Sr 88	
4-8-93	#56PR	22.3	77.7	NC
4-9-93	#56PR	26.8	73.2	1500ppb

NC - not calculated

Support for the LANT Hypothesis

According to Bush's LANT hypothesis[3] ("Lattice Assisted Nuclear Transmutation") strontium production would not necessarily be the end of the transmutation line. Rather, the Sr atoms formed in the lattice would themselves now become targets for the lattice assisted addition of a proton. This would produce an entire cold nucleosynthetic series, the Rubidium Series[3], shown in Fig.7 taken from reference 3.

Figure 7

Isotope Production via Cold Nucleosynthesis: Rubidium Series
(Cell 53)

Mass Number (A)	Nuclides Synthesized	Net number of Nuclei Synthesized x 10^{16}	Total Energy Released (MeV x 10^{17})
86	$_{38}Sr^{86}$	1.34	1.29
87	$_{38}Sr^{87}$	19.25	33.30
88	$_{38}Sr^{88}$, $_{39}Y^{88}$(108D), $_{40}Zr^{88}$(88D)	0.52	0.55
89	$_{39}Y^{89}$	1.66	4.6
90	$_{40}Zr^{90}$	0.28	1.1
91	$_{41}Nb^{91}$	3.00	12.1
92	$_{42}Mo^{92}$	(small)	(small)
93	$_{42}Mo^{93}$	27.03	148.10
94	$_{42}Mo^{94}$	0.23	1.43
95	$_{42}Mo^{95}$	(small)	(small)
96	$_{44}Ru^{96}$, $_{43}Tc^{96}$(4.35D)	(small)	(small)
97	$_{43}Tc^{97}$, $_{44}Ru^{97}$(2.9D)	(small)	(small)
98	$_{44}Ru^{98}$	(small)	(small)
99	$_{44}Ru^{99}$, $_{45}Rh^{99}$(16.1D)	(small)	(small)
100	$_{45}Rh^{100}$, $_{46}Pd^{100}$(4D)	0.30	3.90
101	$_{44}Ru^{101}$, $_{45}Rh^{101}$(3y)	3.70	41.30
102	$_{45}Rh^{102}$, $_{46}Pd^{102}$	1.21	14.50
103	$_{45}Rh^{103}$, $_{46}Pd^{103}$(17D)	1.40	17.80
104	$_{46}Pd^{104}$	0.54	7.30
105	$_{46}Pd^{105}$, $_{47}Ag^{105}$(40D)	(small)	(small)
106	$_{46}Pd^{106}$, $_{48}Cd^{106}$	(small)	(small)
107	$_{47}Ag^{107}$	0.54	7.30
108	$_{48}Cd^{108}$	0.23	3.90
109	$_{47}Ag^{109}$, $_{48}Cd^{109}$(453D)	2.25	39.70
110	$_{48}Cd^{110}$	(small)	(small)
111	$_{48}Cd^{111}$, $_{49}In^{111}$(2.8D)	(small)	(small)
112	$_{50}Sn^{112}$	2.25	44.60
	Sums:	65.73 x 10^{16}	**384.17 x 10^{16} MeV**

Estimating a ten percent error, then, the total energy to produce the above based upon the LANT Model is approximately **(3.8 ± 0.4) x 10^{19} MeV** versus the total excess heat determined from calorimetry for Cell 53 of **(4.0 ± 0.8) x 10^{19} MeV**.

A comparison of the SIMS spectrographs of the cathode material of Cell 53 (rubidium carbonate) before and after running provides evidence for the synthesis of such nuclides as shown in the Table of Fig. 8 entitled "Isotope Production via Cold Nucleosynthesis: Rubidium Series[3]." In this respect it is interesting to note from the Table in Fig. 8 that the total excess heat produced in connection with this synthesis should be (3.8 ± 0.4) x 10^{19} MeV, whereas the actual excess heat for cell 53 as determined from calorimetry[3] was approximately (4.0 ± 0.8) x 10^{19} MeV. This is rather good agreement and provides initial support for the LANT hypothesis.

Evidence for Electrolytically Induced Radioactivity

Fig. 9 displays a radioactive decay curve obtained employing the postrun cathode material of cell 71, a light water rubidium carbonate cell (0.57 M) with nickel mesh cathode and platinum anode that ran for approximately two months.

FIGURE 8

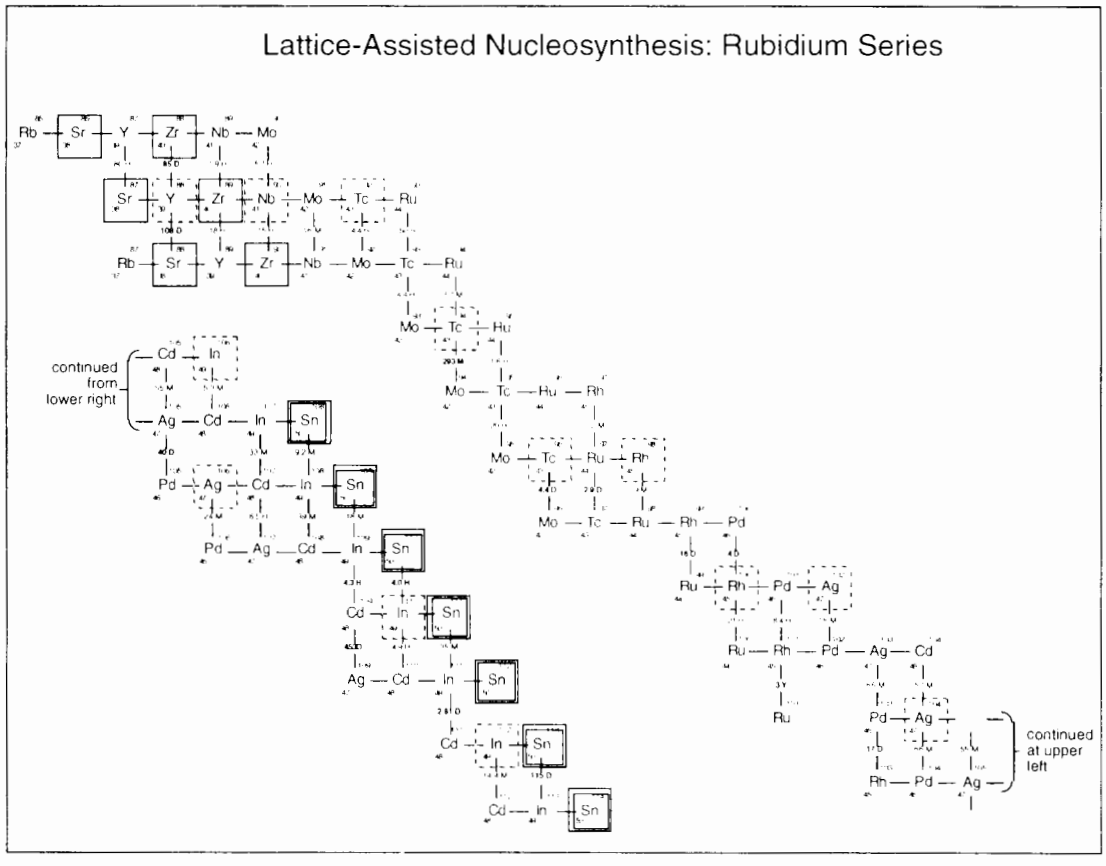

FIGURE 9:

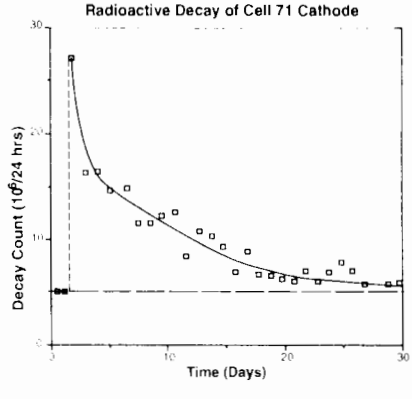

Nine days elapsed betwen the end of electrolysis and the beginning of radiation monitoring with the sample in a lead bunker to reduce background levels. Counting was carried out with a Bicron 1.5 inch diameter NaI scintillation detector encased in a thickness of about one-eighth inch of aluminum. The signal from the scintillation detector was fed into a mulitichannel analyzer employing an 811-3 multichannel analyzer PC board and software by Nucleus, Inc. of Oak Ridge, Tennessee. The counts shown were each taken over a twenty four hour period to even out diurnal background fluctuations and each represents the sum of the counts in the lowest twenty two channels, channel 19 through channel 40, with channel 40 corresponding to an energy of about 20 keV. The first two points of the decay curve in Fig. 9 correspond to two consecutive 24 hour background counts taken in the lead bunker, and were each about 5 million counts. However, once the sample was in place, it was deemed important to monitor the postrun cathode without moving it between the twenty four hour counts. The monitoring for radioactivity continued for about one month as shown, and at which time the count appears to be approaching the background asymptotically. Fig. 10 displays a semi-log plot of count versus time in days yielding a half-life of about 3.8 days.

FIGURE 10:

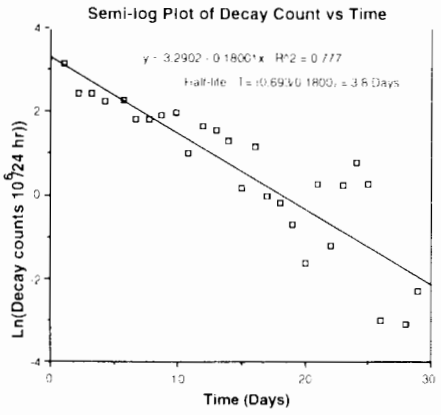

In that regard Bush points out that it is interesting that a simple unweighted average of the half-lives for the short-lived radionuclides deduced by Bush from his LANT Hypothesis[3] (See Fig. 8) for his hypothesized Rubidium Series[3] (Fig. 7) and from the SIMS analysis for cell 53 (rubidium carbonate) yields an average half-life of 3.5 days: (From Fig. 8) Tc-96 (4.35 D), Ru-97 (2.90 D), Pd-100 (4.0 D), and In-111 (2.8 D). Also, possibly related to this is the fact that a "down" data point on the decay curve, meaning one that was lower than the previous twenty four hour count , was usually followed by one or more points where the count stayed the same, or increased. Whether this indicates that a larger standard devistion (error bar) on the order of ±3,000,000 counts in a 24 hour period is more appropriate than the ±1,000 count error bar used, or whether this represents an additional phenomenon of interest such as the emergence of tritium from the sample is not clear at this stage. At any rate, Bush notes that if he employs just the "down" (decreasing count) data points that the half-life of the decay curve is equal to the 3.5 days indicated above, and this is displayed in the semi-log plot of Fig. 11.

FIGURE 11:

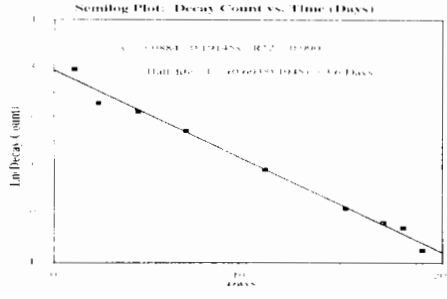

(Fig. 12 portrays a plot of average half-life versus channel number based upon the first twenty days of counting, and is consistent with the average half-life for the sum of the twenty four hour counts for the first twenty two channels of about 3.8 days.) So far as we know, this data constitutes the first reported results for radioactivity associated with measurement for cathode material removed from the electrolytic cell. We had previously reported[5] x-ray detection in the case of an LiOH cell with a nickel mesh cathode measured while the cell was running, and for an LiOD cell with a palladium cathode measured following the end of electrolysis but measured with the electrode in place in the cell.

FIGURE 12:

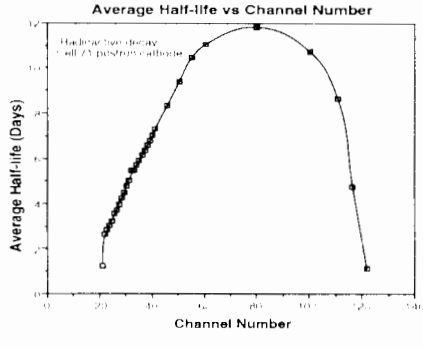

Conclusions

With the corroborative independent mass spectrographic results of the two separate laboratories the evidence supporting the electrolytically induced transmuation of rubidium to strontium, as evidenced by the shift in the abundance ratio or Sr-86 to Sr-88, must be considered very strong. These results add support to Bush's CAF and LANT hypotheses. Note that any strontium contamination would only tend to shift this ratio back to the natural abundance ratio for the two strontium isotopes. If these results can be corroborated by independent observers, they should stand as one of the high water marks of cold fusion research. The evidence for electrolytically induced radioactivity in a rubidium cell as monitored outside the cell by a scintillation counter after the discontinuation of electrolysis represents another breakthrough if it can be independently verified.

Acknowledgments

T. Passell (EPRI) is thanked for his encouragement and for his interest in the Cal Poly project. ENECO, formerly FEAT, is thanked for its financial support and encouragement. M. Hovanec of West Coast Analytical Service, Inc. (Santa Fe Springs, CA) is greatly appreciated for the independent, and first rate, ICPMS mass spectroscopy. Finally, thanks go to Bernice Gilbert of the Cal Poly (Pomona) Instructional Support Center for her help in preparing the manuscript.

References

1. R. Bush, "A Light Water Excess Heat Reaction Suggests that 'Cold Fusion' May Be 'Alkali-Hydrogen Fusion' ", Fusion Technol., 22, 301 (1992).
2. R. Bush and R. Eagleton, "The Transmission Resonance Model for Cold Fusion in Light Water: I. Correlation of Isotopic and Elemental Evidence with Excess Power", Proc. 3-ICCF, 409,(1993).
3. R. Bush, "Towards a Nuclear Physics of Condensed Matter", accepted for Fusion Technol., under revision, est. issue: March'94.
4. R. Bush and R. Eagleton, "Calorimetric Studies For Several Light Water Electrolytic Cells With Nickel Fibrex Cathodes and Electrolytes With Alkali Salts of Potassium, Rubidium, and Cesium", submitted to Proc.4-ICCF (1994).
5. R. Bush and R. Eagleton, "Experimental Studies Supporting the Transmission Resonance Model for Cold Fusion in Light Water: II. Correlation of X-Ray Emission with Excess Power", Proc. 3-ICCF, 409 (1993).
6. R. Bush, "Will the Light Water excess Heat Effect Lead to a Unification with Cold Fusion?", Twenty First Century Science and Technology, Fall 1993, p. 75.

* Both this manuscript and that of ref. 4 were selected to be included in these refereed Transactions, although in the form of a single manuscript. Due to time limitations, the authors decided against this.

** University of Utah Research Park, 391-B Chipeta Way, Salt Lake City, Utah 84108.

Appendix A: Interpretation of the SIMS Mass Spectrograms

The mass spectrograms of Fig. 2 and Fig. 3 were carried out by SIMS analysis, respectively, for the postrun cathode material and for the prerun cathode. (Earlier mass spectrometry established an upper limit on the strontium in the post-run solution from cell 53 of 5 ppb.) Note the following from Fig. 3 (Prerun):

Fig. 3 (Prerun): Mass 86: The height of this signal is about 3.6 cm corresponding on the log-scale to an ordinate of 190 counts.
3.5 cm signal height: 150 counts

Nickel 58: 10.0 cm signal height: 1,250,000 counts
Fig. 2 (Postrun): Note that the signal height discrimination for this spectrogram is greater than that for the one of Fig. 3. Thus, the spectrogram of Fig 3 is associated with only a 50 V offset, whereas that of Fig. 2 is associated with a 125 V offset. Thus, in comparing signal heights from Fig. 2 to those on Fig. 3 we must multiply the numbers of counts in Fig. 2 by the ratio of the Nickel 58 signal in Fig. 3 to that in Fig. 2:

Mass 86: 3.25 signal height: 36 counts

Mass 88: 2.6 cm signal height: 16 counts

Nickel 58: 9.5 cm signal height: 31,000 counts

Ratio of Nickel 58 signal in Fig.3 to that in Fig.2: (1,250,000/ 31,000)= 40.32.

Corrected counts from Fig.2 to compare with those in Fig.3:

Mass 86: 36 x 40.32 = 1, 452 counts

Mass 88: 16 x 40.32 = 645

Ratio of Sr-86 to Sr-88: (Corrected for background in Fig.3):

$$(1{,}452 - 190)/(645 - 150) = 2.55. \quad (1)$$

Note that the ratio of the natural abundances of Sr-86 and Sr-88 is approximately:

$$0.12 \quad (2)$$

Thus, we have an isotopic abundance ratio shift by a factor of

$$2.55/0.12 = 21. \quad (3)$$

Note, also, that the ratio of the natural abundances of Rb-85 and Rb-86 is about

$$2.59. \quad (4)$$

The fact that the ratio in (1) so closely matches that in (4) is strong support for Bush's hypothesis that the strontium arises from the rubidium via the addition of a proton at the surface of the nickel.

Finally, how do we know that masses 86 amd 88 in B correspond to strontium and not, say, to rubidium hydride. Quite aside from the well-known instability of rubidium hydride is the fact that a second mass spectrometric study in which the rubidium and strontium are first chemicaly separated via an ion exchange column shows a strong enhancement of Sr-86 over Sr-88 both for the post-run cathode material of cell 53 and for a new light water rubidium hydroxide (0.57 M) cell (cell 56).

Appendix B: (WCAS)

WEST COAST ANALYTICAL SERVICE, INC.

C.S.P.U. **Job # 23653**
Dr. Robert T. Bush **April 22, 1993**

LABORATORY REPORT

Text

Strontium Isotope Ratio Determination

Summary

The results obtained and listed in Table 1 show that the method works as designed, using single and mixed standards. For sample A#53, some enhancement was determined, particularly on 4-9-93 when sequence 2 was performed, Sr86 = 22.2±0.05. Sequence 2 has been producing the most consistent results. Sample #56PR demonstrated verifiable enhancement, Sr86 = 26.8±0.05.

On 4-14-93, we decided to run A#53W1 from the first sequence just to have similar batch results as obtained for #56PR. The strontium standard looks great; not much strontium detected in the sample. (Pages 50 and 9.)

The next experiment was designed to improve the chromatography. The amount of rubidium in solution exceeds the capacity of one column, so two columns were hooked together and a series of solutions run through them. The results for the standard are very consistent with single column values; however, for a real sample such as A#53, the strontium is still coming out early in W1 instead of DP-2 where we would like it to. (See pages 51 and 52, also results pages 10 and 11, 4-15-93.)

To demonstrate adequate resolution of the mass spectrometer, an experiment was devised on 4-16-93 (page 53). The idea is to use the scanning mode on the ICPMS instead of the peak jumping mode used when measuring isotope ratios. In the scanning mode, the resolution between peaks would be more obvious because many more data points are taken as the mass spec scans through the mass ranges. This test was run twice because the detector tripped off due to the high rubidium counts. For the second scan, the autotrip function was overridden. Page 12 shows the trip results while page 13 shows the scan with the trip switched off. The results are most vividly shown in the two mass spectra, page 14 and 15. Page 14 shows excellent base-line resolution and demonstrates the difference in magnitude of the rubidium/strontium concentrations.

Page 15 shows what would happen to the spectrum and the results if no chromatography was used on the samples to reduce the rubidium levels. Notice peak saturation for both rubidium isotopes as indicated by pitch-fork shaped peaks. Also notice the peak widths and how they spread out into the mass 84 and 87 to some extent.

Page 16 is a mass spectrum of the peak jumping mode, and it shows the resolution, peak width also.

Experimental

Rubidium carbonate impregnated nickel matte electrodes from WCAS Job number 22542 were subjected to ultrasonic cleaning and acid etching to solubilize any strontium isotopes present so isotope ratio measurements using ICPMS could be made. Results are summarized in Table 1. Total Strontium levels were calculated and are reported in Table 1.

Ion Chromatography/cation exchange was used to separate the nonovalent rubidium from the divalent strontium. Ten milliliter fractions were collected from the end of the column and analyzed in batches by ICPMS.

A two-step sample preparation scheme was used. The first step was eight hours of sonication in 2mH HCl. The second step was 24 hours of sonication in 10% HCl, followed by 4 days of room temperature etching with the end point being a light green color from the nickel matrix. Each of the two samples was then washed with DI water three times and set aside to dry. The solutions of 10% HCl were then brought to approximately thirty milliliters (see page 43).

The first analytical sequence (Ion Chromatography, fraction collection, Isotope ratio ICPMS) of the two samples and a strontium only standard is recorded on pages 44 & 45. The actual instrument printouts are on unruled paper, pages 1-3. The results indicate possible enhancement for A#53 and substantial enhancement for #56, data Table 1, 4-8-93.

The second analytical sequence (pages 46 & 47, results pages 4-6) is from sending the fractions collected in sequence one, back through the column to try to get better separation between the rubidium and strontium. The results indicate enhancement for both samples. See results Table 1 data for 4-9-93.

The third sequence came out of our concern for demonstrating that the rubidium levels in the samples were not artificially enhancing the strontium isotopes, resulting in false ratios. (Pages 48 & 49 on 4-13-93 and pages 7 & 8 from printouts contain test information.) The conclusion is that the chromatography is providing enough separation and the resolution of the mass spectrometer is such that no artificial ratio enhancement is being induced by the high rubidium levels. Isotope ratio values are listed in Table 1 for 4-13-93.